MATERIALS PERFORMANCE OF STRUCTURAL ALLOYS IN SIMULATED OXY-FUEL ENVIRONMENTS*

K. Natesan, Z. Zeng, and D. L. Rink
Argonne National Laboratory, 9700 South Cass Avenue, Argonne, IL 60439
E-mail: natesan@anl.gov; Telephone: (630) 252-5103; Fax: (630) 252-8681

June 2010

Paper presented at the 24th Annual Conference on Fossil Energy Materials, Pittsburgh, PA, May 25-27, 2010 and to be published in the conference proceedings.

*Work supported by the U.S. Department of Energy, Office of Fossil Energy, Advanced Research Materials Program, Work Breakdown Structure Element ANL-4, under Contract DE-AC02-06CH11357.

MATERIALS PERFORMANCE OF STRUCTURAL ALLOYS IN SIMULATED OXY-FUEL ENVIRONMENTS*

K. Natesan, Z. Zeng, and D. L. Rink
Argonne National Laboratory, 9700 South Cass Avenue, Argonne, IL 60439
E-mail: natesan@anl.gov; Telephone: (630) 252-5103; Fax: (630) 252-8681

Abstract

The U.S. Department of Energy (DOE) Office of Fossil Energy is intensely promoting research and development of oxy-fuel combustion systems that employ oxygen, instead of air, for burning the fuel. The resulting flue gas primarily consists of H_2O and CO_2 that facilitates sequestration of CO_2 or use it in a turbine to generate electricity, thereby leading to reduction in CO_2 emissions. Also, as the oxidant is bereft of N_2, NO_x emissions are minimized to a great extent from the exhaust gas. Studies at NETL have indicated that oxy-fuel combustion can increase efficiency in the power plants from the current 30-35% to 50-60%. However, the presence of H_2O/CO_2 and trace constituents like sulfur and chlorine in the gas environment and coal ash deposits including alkalis at the operating temperatures and pressures can have adverse effects on the corrosion and mechanical properties of structural alloys. Thus, there is a critical need to evaluate the response of structural and turbine materials in simulated H_2O/CO_2 environments in an effort to select materials that have adequate high temperature mechanical properties and long-term environmental performance.

As a first step, last year we tested coupon specimens of several candidate alloys in pure CO_2 and in CO_2 plus steam environments at temperatures between 650 and 950°C for times up to 10,000 h. Materials selected for the study include intermediate-chromium ferritic steels, Fe-Cr-Ni heat-resistant alloys, and nickel-based superalloys. We presented detailed results on the corrosion performance of various alloys after exposure at 750°C. We also addressed the mechanism for the oxidation of various alloys in these environments and also evaluated the long-term performance of the alloys from the standpoint of scaling and internal penetration. The oxidation test results showed that the total corrosion (scaling plus internal penetration) rates are <0.05 mm/y at 750°C, in the absence of ash or sulfur. During the current year, we conducted tests to evaluate the corrosion performance of the structural alloys in the presence of simulated coal ash consisting of alumina, silica, and iron oxide along with sodium and potassium sulfates. Detailed results are presented on weight change, scale thickness, internal penetration, microstructural characteristics of corrosion products, and cracking of scales for the alloys after exposure at 750°C. To establish the role of steam in the exposure environment, tests were also conducted in environments with and without steam in the oxy-fuel gas atmospheres. Results from these tests are used to address the role of steam in the long-term corrosion performance of alloys.

Background

An increase in carbon dioxide gas in the atmosphere is identified as one of the major causes for the global climate change and one of the sources of carbon dioxide is the exhaust from fossil fuel fired combustion power plants. The energy production, in particular electricity generation, is expected

to increase globally due to population increase and per capita increase in energy consumption. To meet the energy needs, fossil fuels (coal, oil, and gas) will play a major part in production even with a projected increase in alternate renewable sources. However, to minimize the carbon dioxide emission, the current systems emphasize its capture from power plants and subsequent sequestration. The oxy-fuel combustion systems (without the diluent nitrogen gas) can enable recycling of the carbon dioxide to the compressor, use of novel gas turbines, and advance reuse.
The U.S. department of Energy/Office of Fossil Energy is supporting the development of combustion systems replacing air with nearly pure oxygen with a goal to achieving a near zero-emission coal-based power system. For this purpose turbines and combustor technologies that use pure oxygen in fuel combustion are being developed. The major advantage of combustion under pure oxygen is the potential for separation and capture of CO_2 and for achieving power system efficiencies in the range of 50 to 60%.

As a first step, last year we evaluated the corrosion performance of candidate materials in CO_2, steam, steam-CO_2 mixtures, and air [1-3]. Materials selected for the study include intermediate-chromium ferritic steels, Fe-Cr-Ni heat-resistant alloys, and nickel-based superalloys. Coupon specimens of several of the alloys were exposed to pure CO_2 and to CO_2 plus steam environments at temperatures between 650 and 950°C for times up to 10,000 h. We presented detailed results on the corrosion performance of various alloys after exposure at 750°C. The data showed that the weight change for all the alloys was small when tested in all four environments. Among the alloys, Alloy 800 exhibited the most weight gain in all four environments. In general, high nickel and Ni-base alloys exhibited less oxidation than the Fe-base alloys in all exposure environments. The high silicon alloys such as Alloys 330 and 333 showed superior corrosion resistance in pure CO_2 environment when compared their performance in CO_2-steam or pure steam environments. The volatilization of silicon oxides in steam-containing environments may be the cause for this increased corrosion. We also addressed the mechanism for the oxidation of various alloys in these environments and also evaluated the long-term performance of the alloys from the standpoint of scaling and internal penetration. The oxidation test results showed that the total corrosion (scaling plus internal penetration) rates are <0.05 mm/y at 750°C, in the absence of ash or sulfur.

During the current year, we conducted tests to evaluate the corrosion performance of the structural alloys in the presence of simulated coal ash consisting of alumina, silica, and iron oxide along with sodium and potassium sulfates. Detailed results are presented on weight change, scale thickness, internal penetration, microstructural characteristics of corrosion products, and cracking of scales for the alloys after exposure at 750°C. To establish the role of steam in the exposure environment, tests were also conducted in environments with and without steam in the oxy-fuel gas atmospheres. Results from these tests are used to address the role of steam in the long-term corrosion performance of alloys.

Experimental Procedure

Materials

The compositions of the alloys selected for the study are listed in Table 1. Several alloys, both ASME coded and uncoded, were selected for corrosion evaluation. The alloys included advanced ferritic steel modified 9Cr-1Mo and austenitic Fe-base alloys Types 304 and 330

stainless steel and Alloy 800H. In addition, several high-Ni alloys (333, 617, 625, 602CA, 230, 693, 740, and 718) were included in the study, especially for application at temperatures above 700°C. MA956 is a Fe-Cr alloy produced via mechanical alloying and subsequent extrusion.

Apart from fireside and steam side corrosion resistance, the alloy selected for application in steam superheaters and reheaters should possess adequate strength at elevated temperatures for the duration of service. Figure 1 shows a compilation of ASME Code allowable stress values as a function of temperature. Figures 1(a) and 1(b) show the stress values for 460-900°C and 650-800°C, respectively. Alloys such as 693, 740, and MA956 are not Code certified and their stress values are not shown in the figures. However, laboratory creep test data indicate that Alloy 740 has higher strength than those of Alloys 617 or 230.

Table 1. Nominal composition (in wt.%) of alloys selected for corrosion study

Material	C	Cr	Ni	Mn	Si	Mo	Fe	Other
Modified 9Cr	0.10	9.0	0.8	0.5	0.4	1.0	Bal	Nb 0.08, V 0.20, N 0.06
304	0.08	18.0	8.0	1.6	0.6	-	Bal	
800H	0.08	20.1	31.7	1.0	0.2	0.3	Bal	Al 0.4, Ti 0.3
330	0.05	10.0	35.0	1.5	1.25	-	Bal	
333	0.05	25.0	45.0	-	1.0	3.0	18.0	Co 3.0, W 3.0
617	0.08	21.6	53.6	0.1	0.1	9.5	0.9	Co 12.5, Al 1.2, Ti 0.3
625	0.05	21.5	Bal	0.3	0.3	9.0	2.5	Nb 3.7, Al 0.2, Ti 0.2
602CA	0.19	25.1	62.6	0.1	0.1	-	9.3	Al 2.3, Ti 0.13, Zr 0.19, Y 0.09
230	0.11	21.7	60.4	0.5	0.4	1.4	1.2	W 14, Al 0.3, La 0.015
693	0.02	28.8	Bal	0.2	0.04	0.13	5.8	Al 3.3, Nb 0.67, Ti 0.4, Zr 0.03
740	0.07	25.0	Bal	0.3	0.5	0.5	1.0	Co 20.0, Ti 2.0, Al 0.8,, Nb+Ta 2.0
718	-	19.0	52.0	-	-	3.0	19.0	Nb 5.0, Al 0.5, Ti 0.9, B 0.002
MA956	-	20.0	-	-	-	-	Bal	Al 4.5, Ti 0.5, Y_2O_3 0.6

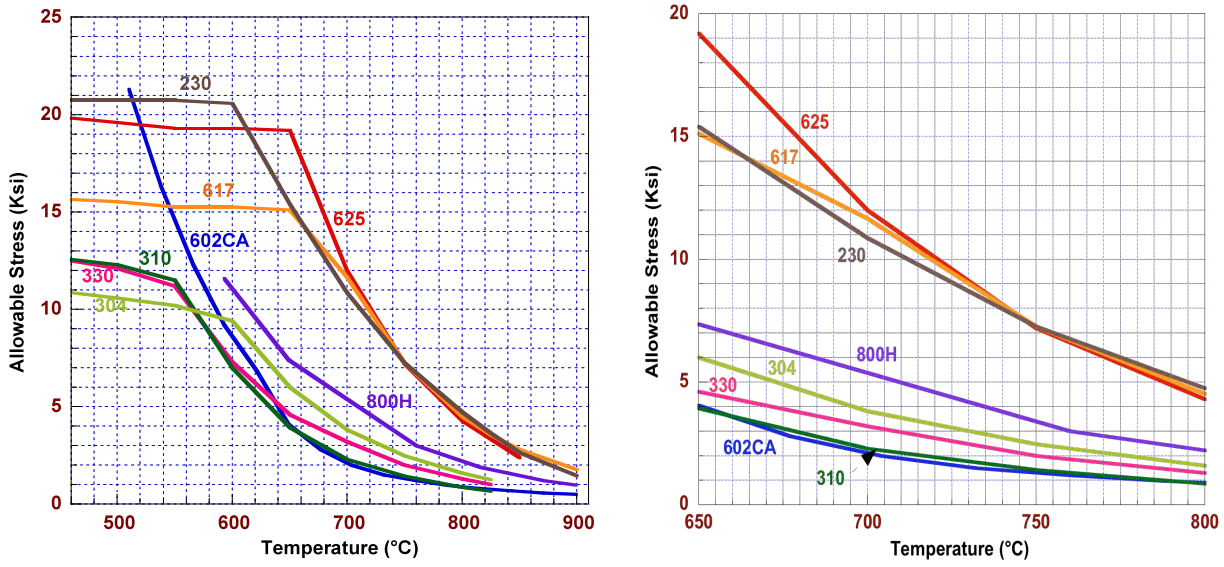

(a) (b)

Figure 1. Code allowable stress as a function of temperature for various structural alloy candidates for the temperature range (a) 460-900°C and (b) 650-800°C.

Synthetic Ash Experiments

The synthetic coal-ash deposit consisted of a mixture of reagent-grade SiO_2, Al_2O_3, and Fe_2O_3 in the ratio of 1:1:1 by weight. The alkali sulfate mixture consisted of Na_2SO_4 and K_2SO_4 in the ratio of 1:1 by weight. The specimens were buried in the ash that was contained in an alumina boat. The experiments were generally stopped after 300 h, and the specimens were cooled to room temperature, cleaned of the ash by brushing, and weighed. Specimen exposures were continued with a fresh supply of ash mixture. The specimen temperature was controlled to within ≈3°C.

Upon completion of the corrosion kinetics experiments, the specimens were examined by optical metallography and by a scanning electron microscope (SEM) equipped with energy–dispersive X–ray analyzer. In some cases, the deposit materials and the scales (developed on alloy specimens) were analyzed by X-ray diffraction. Optical examination of cross sections of exposed specimens and analyses with the SEM were used to identify the morphological features of corrosion-product phases in the scale layers and to establish the thickness of scales and depth of intergranular penetration, if any, in the alloys.

Results and Discussion

Performance in the absence of Ash constituents

Specimens of various alloys were exposed to pure CO_2, 50% CO_2-steam, and air at 750°C and in pure steam at 725°C, for times up to 10,090 h. Among the alloys, Alloy 800 exhibited the most weight gain all four environments. In general, high nickel and Ni-base alloys exhibited less oxidation than the Fe-base alloys in all exposure environments. The high silicon alloys such as Alloys 330 and 333 showed superior corrosion resistance in pure CO_2 environment when compared their performance in CO_2-steam or pure steam environments. The volatilization of silicon oxides in steam-containing environments may be the cause for this increased corrosion.

Figure 2 shows a plot of the relative stability of various oxide and spinel phases as a function of temperature. Also shown in the figure are the oxygen partial pressures established by the CO_2 and steam environments. It is evident that all the relevant (to alloy protection) oxide and spinel phases will be thermodynamically stable in both exposure environments. Therefore, the phases that form in the thermally grown scale will be influenced predominantly by the alloying elements present in the alloy rather than by the oxygen partial pressure in the exposure environment.

The exposed specimens were also analyzed to evaluate the total corrosion (scale thickness and penetration) for all the alloys after exposure at 750°C in pure CO_2 and in 50% CO_2–50% steam. Figure 3 shows the scale and penetration rates for several alloys tested at 750°C in 50% CO_2–50% steam environment, assuming a parabolic kinetics. Results showed that all of the alloys exhibit total corrosion rate of <0.05 mm/y at 750°C. The measured corrosion rates include penetration depth values that were observed in the pits and represent maximum rates for these alloys. Figure 4 shows the ratio of penetration depth to scale thickness observed for alloys tested at 750°C in 50% CO_2–50% steam and in pure CO_2. The data indicate that the penetration rates are much grater than

the scaling rates (ratio being >1) and such increased penetration of the alloy can affect the long-term mechanical property (such as creep and creep fatigue) of the structural components.

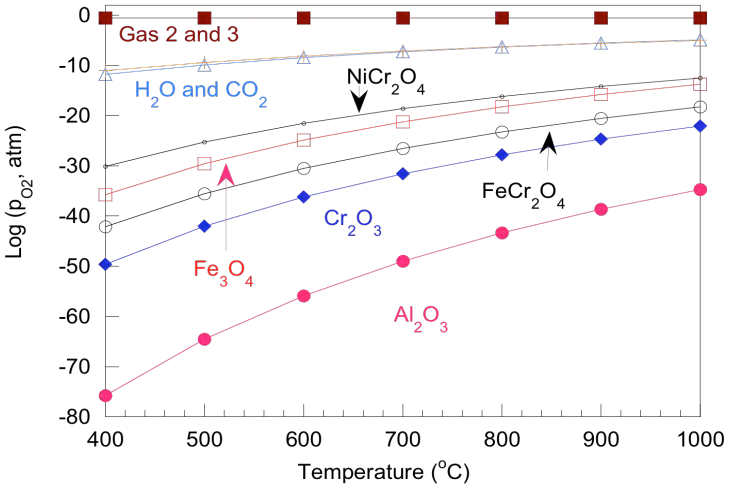

Figure 2. Thermodynamic stability of various oxide and spinel phases. Also shown are the pO_2 curves for pure CO_2 and pure steam.

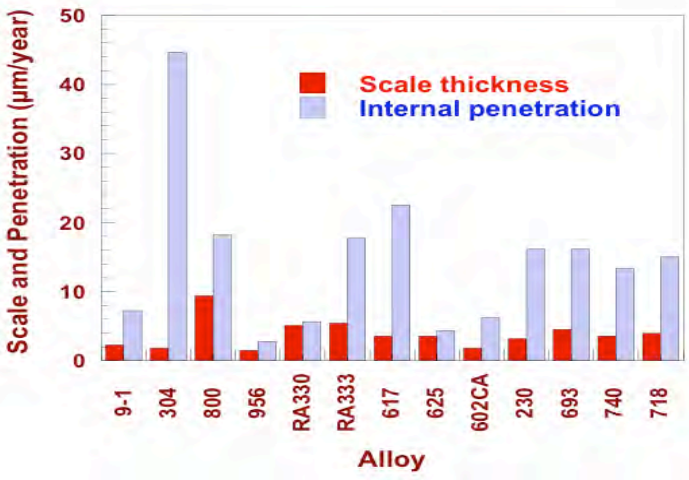

Figure 3. Scale and penetration rates for alloys tested in 50% CO_2-50% steam at 750°C.

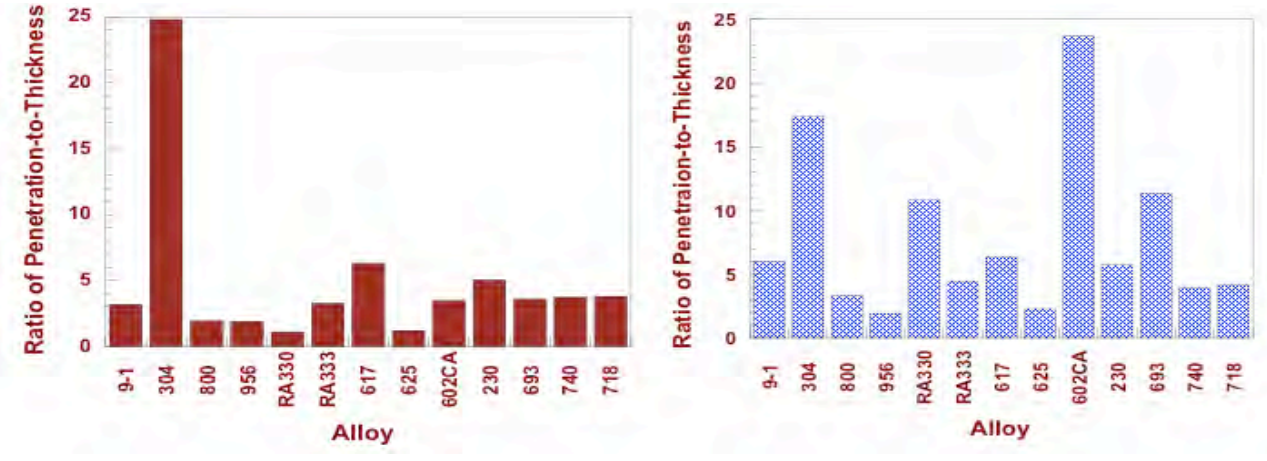

(a) (b)

Figure 4. Ratio of penetration depth to scale thickness for alloys exposed at 750°C to (a) 50% CO_2-50% steam and (b) pure CO_2.

Figure 5 shows the effect of exposure time on the relative alloy penetration rate to the scaling rate for the alloys exposed to pure CO_2 environment. The results show that the internal penetration rates are much larger than the scaling rates for most of the alloys. The penetration-to-thickness ratios for alloys MA956, 740 and 718 are close to 1, indicating that scaling and penetration rates are almost time independent and both progress at the same rates. Many of the other alloys exhibit penetration-to-thickness ratios >1 with increased exposure time, and this may have implications on the long-term mechanical properties of the alloys. In such cases, a simple corrosion allowance to account for metal wastage may not be realistic to assess and account for the corrosion degradation.

The effect of Cr content of the alloy on the corrosion performance of alloys in environments with and without steam was examined. Figure 6 shows the weight loss data for the alloys in pure CO_2 environment at 750°C. Chromium content itself has very little effect on the corrosion performance of an alloy as long as the concentration is >20 wt.%. The mechanically alloyed MA956 (an alumina former) is an exception in that the alloy corrodes heavily in the presence of steam even though it contains 20 wt.% Cr.

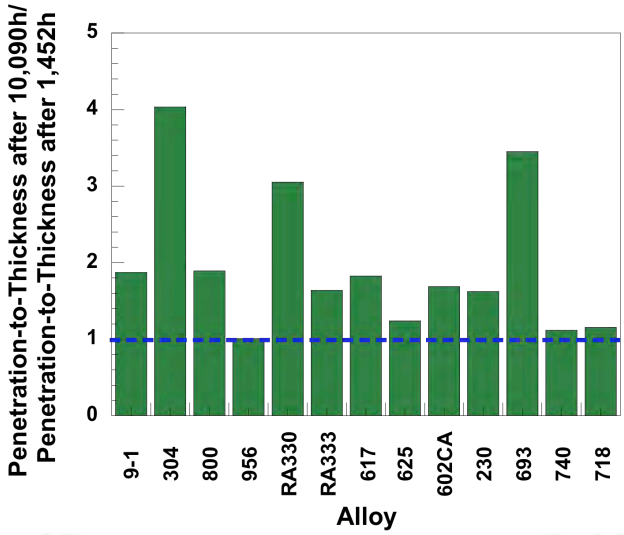

Figure 5. A comparison of the ratio of penetration depth to scale thickness for alloys exposed for 1,452 and 10,090 h in pure CO_2 at 750°C.

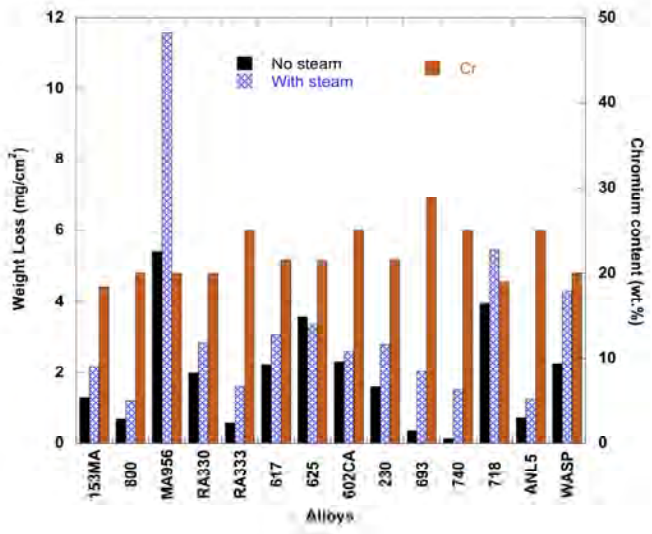

Figure 6. Effect of chromium concentration in the alloys on the weight loss data after exposure in environments with and without steam.

Performance in the presence of Ash constituents

Corrosion experiments in the presence of simulated coal ash and alkali sulfates was conducted at 750°C for a total exposure time of 1200 h. Specimens were weighed periodically and the ash was replenished every 300 h of exposure. Figure 7 shows a macrophotograph of the alloys exposed to coal ash environment and in gas environments with and without steam. Figure 8 shows the weight loss data and maximum corrosion depth for all the alloys tested at 750°C.

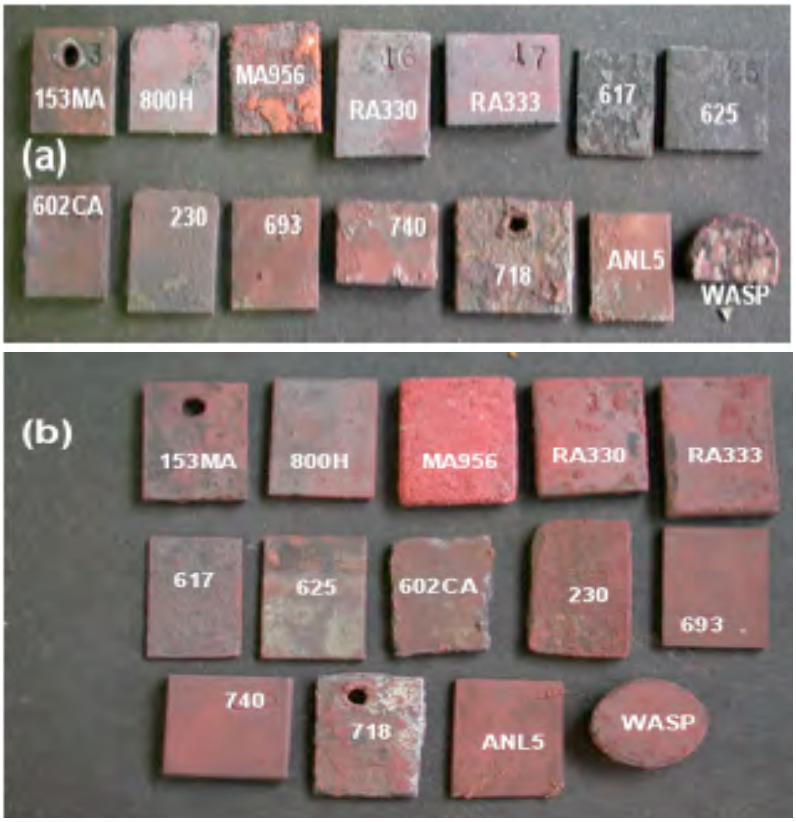

Figure 7. Macrophotograph of specimens in coal ash after 600-h exposure at 750°C in gas environment that contained (a) steam and (b) no steam.

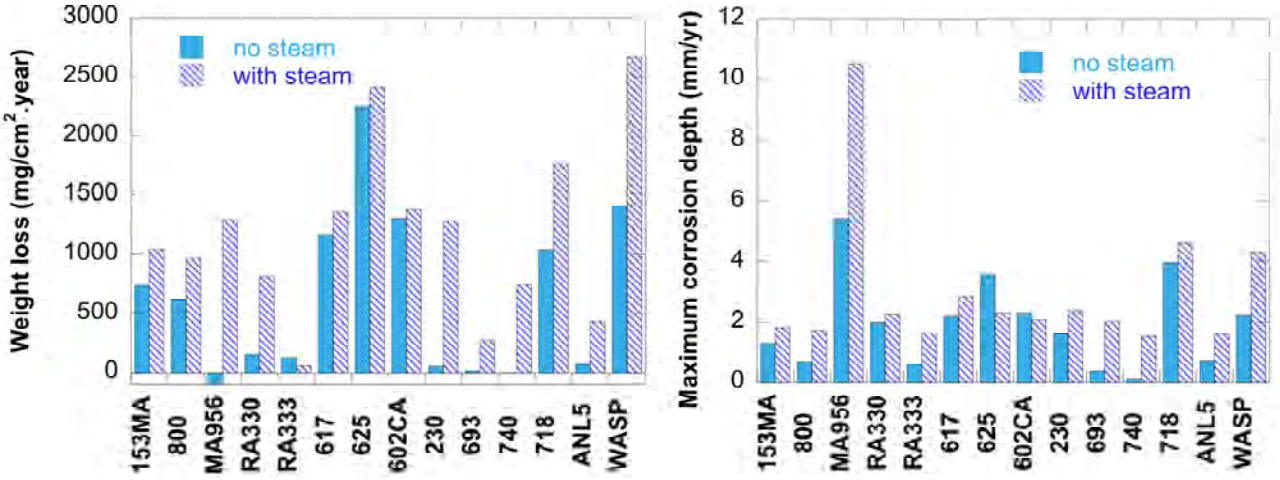

Figure 8. Weight loss and corrosion depth data for various alloys tested in oxy-fuel environment containing simulated coal ash at 750°C.

Figure 9 shows a comparison of corrosion depth for various in simulated oxyfuel environments with and without ash. It is evident that in the absence of ash and sulfates, the alloys exhibit negligible (<30 μm/year) oxidation scaling in the gas environment. In the presence of ash and alkali sulfates, the corrosion rates increase significantly. The observed rates for most of the alloys are >1 mm/year. The presence of steam in the environment, which is typical of oxy-fuel systems, the rates are generally higher (>2 mm/year). Gas turbine alloys such as 718 and Waspaloy and mechanical alloyed MA956 (alumina former) exhibited corrosion rates in the range of 4-11 mm/year.

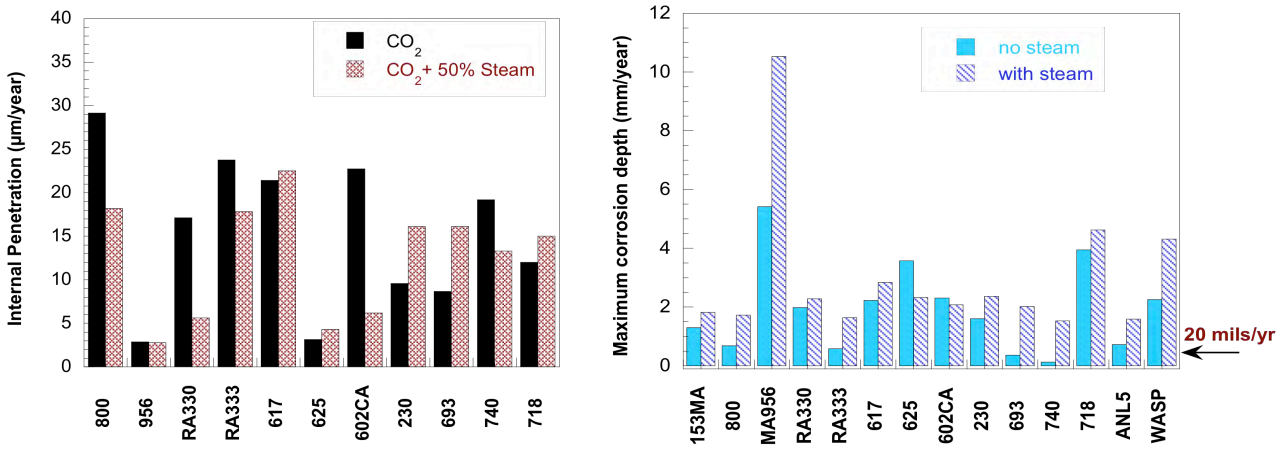

(a) (b)

Figure 9. Corrosion depth data for various alloys tested in oxy-fuel environment at 750°C (a) without ash and (b) with simulated coal ash and alkali sulfates.

Microstructural Characterization of Corrosion Product Phases

The microstructural characteristics of corrosion product phases on several alloys exposed to environments in the absence of ash and alkali sulfates were presented in an earlier published paper (3) and will not be discussed further in this paper. A comparison of the observed corrosion rates with and without ash in the exposure environment shows factors of 50-100 times higher rate in the presence of ash (see Fig. 9). The ash-exposed specimens were analyzed in detail to establish the stability of oxide scales and the extent of sulfidation of the underlying substrates. Microstructural details on a chromia-forming alloy (Alloy 740) and an alumina-forming alloy (MA956) are presented in this paper. In addition, the influence of steam in the exposure environment on the scaling behavior is also presented.

When tested in the environment containing ash and gas without steam, the chromia-forming Alloy 740 developed several pits on the specimen surface. The specimen cross sections in regions with and without pits were analyzed using a scanning electron microscope (SEM) and associated energy-dispersive X-ray analyzer. Figure 10 shows the SEM image and elemental mapping for O, S, Cr, Co, Al, Nb, Ni, and Si in the non-pit region of an Alloy 740 specimen after 1200-h exposure at 750°C in ash and the gas without steam. In the non-pit region, the external scale is predominantly chromium-rich oxide with internal precipitates of Nb sulfides and (Al, Si) oxides. Figure 11 shows the SEM image and elemental mapping for O, S, Cr, Co, Al, Nb, Ni, and Si in the pit region of the Alloy 740 specimen after 1200-h exposure at 750°C in ash and the gas without

steam. It is evident that the scale is a mixture of Cr oxide and Cr sulfide, indicating non-protective nature of the external scale to continued sulfidation.

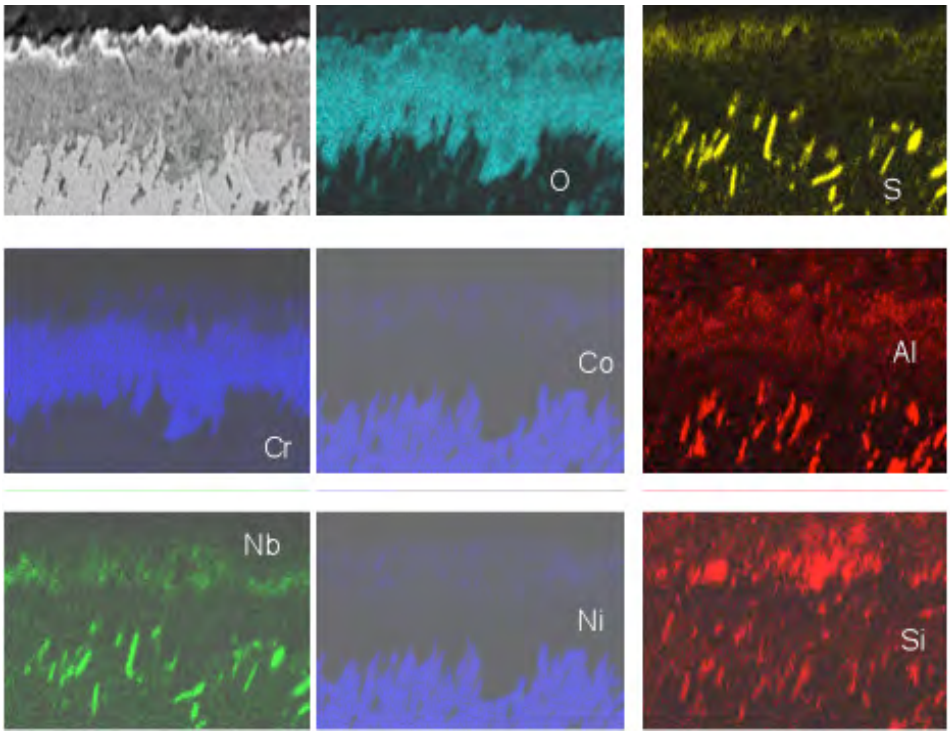

Figure 10. Alloy 740 **non-pit area**, after 1200-h exposure to ash and gas without steam at 750ºC.

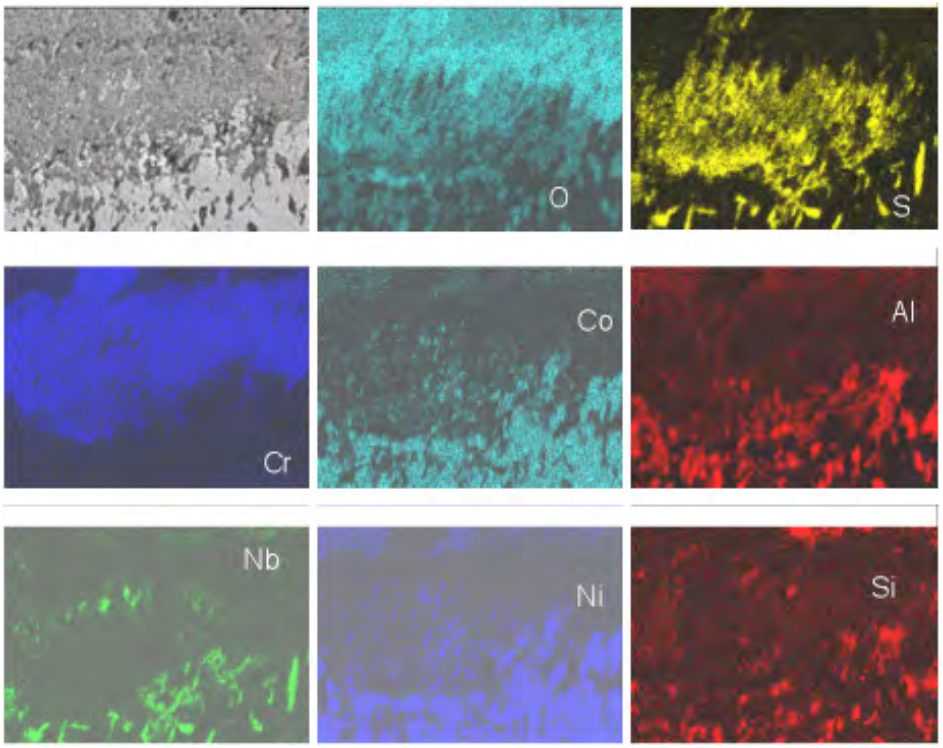

Figure 11. Alloy 740 **pit area**, after 1200-h exposure to ash and gas without steam at 750ºC.

Figure 12 shows the SEM image and elemental mapping for O, S, Cr, Co, Al, Nb, Ni, and Si of an Alloy 740 specimen after 1200-h exposure at 750°C in ash and the gas with steam. Extensive pitting attack was observed and the EDX analysis indicates massive sulfidation attack and the external scale is a mixture of oxides and sulfides of Cr, Al, and Nb. The results indicate that the corrosive attack is catastrophic and is non-reversible and a viable alloy should be resistant to sulfidation in these environments.

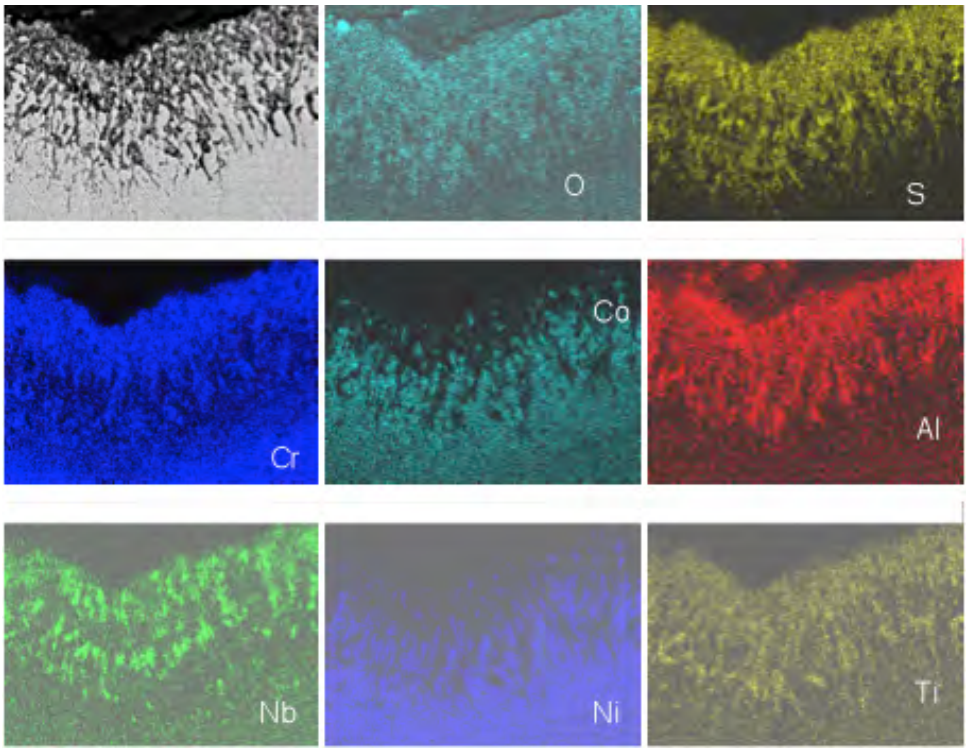

Figure 12. Alloy 740 after 1200-h exposure to ash and gas with steam at 750ºC.

Figure 13 shows the SEM image and elemental mapping for O, S, Cr, Fe, Al, Na, Co, and Si for an Alloy MA956 specimen after 1200-h exposure at 750°C in ash and the gas without steam. Even though the scale looks intact, the scale consists of both oxides and sulfides. Some sodium enrichment is detected at the scale/alloy interface. The corrosion rate observed for this alloy, even without steam in the gas, was 5.5 mm/year (see Fig. 9b) and extremely high. The results show that alumina-forming alloys may not be viable candidates for application in coal ash environments.

Summary

We have conducted a detailed study at Argonne National Laboratory, to evaluate the oxidation performance of structural alloys in CO_2 and CO_2-steam environments at temperatures up to 1000°C. We believe the corrosion rates in these environments (in the absence of sulfur) are acceptable for service. However, the effect on mechanical properties is not established.

Results indicate that the oxide scales that develop on the alloys are not that protective and internal carburization of the substrate may occur.

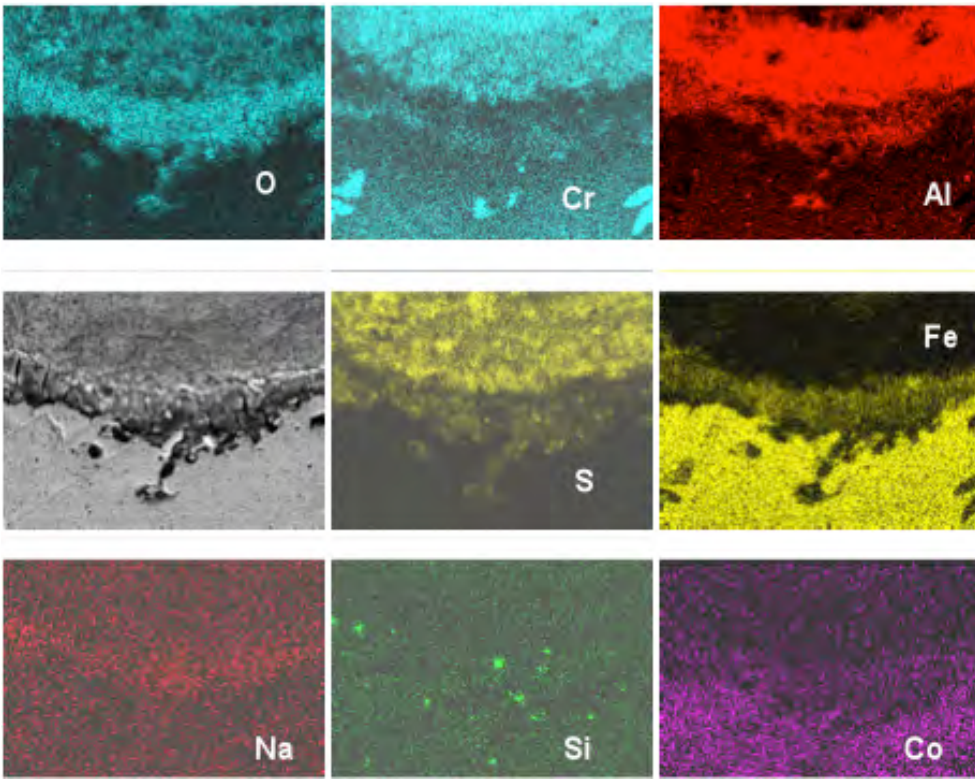

Figure 13. MA956 after 1200-h exposure to ash and gas without steam at 750ºC.

The presence of ash (with alkali sulfates) coupled with steam in the gas environment accelerates corrosion of all structural alloys. Ash-test results show that in the absence of steam, Alloys 800H, 333, 693, 740, and ANL5 exhibit acceptable performance. In the presence of steam, all the alloys exhibit corrosion rates ≥ 2 mm/year, based on linear kinetics.

References

1. K. Natesan and D. L. Rink, "Corrosion Performance of Structural Alloys for Oxy-fuel Combustion Systems," Proc. 21st Annual Conference on Fossil Energy Materials, Knoxville, TN, April 30- May 2, 2007.

2. K. Natesan, Z. Zeng, and D. L. Rink, "Materials Performance of Structural Alloys in CO_2 and in CO_2-Steam Environments," Proc. 22nd Annual Conference on Fossil Energy Materials, Pittsburgh, PA, June 8-10, 2008.

3. K. Natesan, Z. Zeng, and D. L. Rink, "Materials Performance of Structural Alloys in CO_2 and in CO_2-Steam Environments," paper presented at the 23rd Annual Conference on Fossil Energy Materials, Pittsburgh, PA, May 12-14, 2009 and published in the conference proceedings.